



# 1 **Insights into the role of dicarboxylic acid on CCN activity:** 2 **implications for surface tension and phase state effects**

3 Chun Xiong<sup>1</sup>, Binyu Kuang<sup>1</sup>, Xiaolei Ding<sup>3</sup>, Xiangyu Pei<sup>1</sup>, Zhengning Xu<sup>1</sup>, Huan Hu<sup>3\*</sup>, Zhibin Wang<sup>1,2,4\*</sup>

4 <sup>1</sup>College of Environmental and Resource Sciences, Zhejiang University, Zhejiang Provincial Key Laboratory of Organic  
5 Pollution Process and Control, Hangzhou, China

6 <sup>2</sup>ZJU-Hangzhou Global Scientific and Technological Innovation Center, Hangzhou, China

7 <sup>3</sup>Zhejiang University-University of Illinois at Urbana-Champaign Institute, International Campus, Zhejiang University,  
8 Haining 314400, China

9 <sup>4</sup>Key Laboratory of Environment Remediation and Ecological Health, Ministry of Education, Zhejiang University, Hangzhou,  
10 China

11 *Correspondence to:* Zhibin Wang ([wangzhibin@zju.edu.cn](mailto:wangzhibin@zju.edu.cn)) and Huan Hu ([huanhu@intl.zju.edu.cn](mailto:huanhu@intl.zju.edu.cn))

12 **Abstract.** Dicarboxylic acids are ubiquitous in atmospheric aerosol particles, but their roles as surfactants in cloud  
13 condensation nuclei (CCN) activity remain unclear. In this study, we investigated CCN activity of inorganic salt (sodium  
14 chloride and ammonium sulfate) and dicarboxylic acid (including malonic acid (MA), phenylmalonic acid (PhMA), succinic  
15 acid (SA), phenylsuccinic acid (PhSA), adipic acid (AA), pimelic acid (PA) and octanedioic acid (OA)) mixed particles with  
16 varied organic volume fraction (OVF), and then directly determined their surface tension and phase state at high relative  
17 humidity (over 99.5%) by atomic force microscopy (AFM). Our results showed that CCN derived  $\kappa_{\text{CCN}}$  of studied dicarboxylic  
18 acids ranged in 0.003-0.240. A linearly positive relation between  $\kappa_{\text{CCN}}$  and solubility was obtained for slightly dissolved species,  
19 while negative relation was found between  $\kappa_{\text{CCN}}$  and molecular volume for highly soluble species. For most inorganic  
20 salt/dicarboxylic acid (MA, PhMA, SA, PhSA and PA), a good closure within 30% relative bias between  $\kappa_{\text{CCN}}$  and chemistry  
21 derived  $\kappa_{\text{Chem}}$  were obtained. However,  $\kappa_{\text{CCN}}$  values of inorganic salt/AA and inorganic salt/OA systems were surprisingly 0.3-  
22 3.0 times higher than  $\kappa_{\text{Chem}}$ , which was attributed to surface tension reduction as AFM results showed that their surface tensions  
23 were 20%-42% lower than that of water (72 mN m<sup>-1</sup>). Meanwhile, semisolid phase states were obtained for inorganic salt/AA  
24 and inorganic salt/OA and may also affect hygroscopicity closure results. Our study highlights that surface tension reduction  
25 should be considered to investigate aerosol-cloud interactions.

## 26 **1 Introduction**

27 Atmospheric particles can indirectly affect global climate through their impact on aerosol-cloud interaction by serving as cloud  
28 condensation nuclei (CCN) (Rosenfeld et al., 2014). Exploring the factors affecting CCN activation could help to understand  
29 the aerosol-cloud interactions and thus decrease the uncertainty in the assessment of climate model. Köhler theory provides  
30 the basis for linking CCN activity with aerosol thermodynamic properties (Köhler, 1936), in which size and chemical  
31 composition are key factors to determine the activation of aerosol particles. Previous studies pointed out that aerosol number



32 size distribution is essential to determine CCN concentration other than composition (Dusek et al., 2006; Gunthe et al., 2009;  
33 Rose et al., 2010). The role of particle chemistry in the activation process, however, is still debatable due to the complexity of  
34 chemical constitution.

35 Single parameter  $\kappa$  was introduced in Köhler theory to describe hygroscopicity of aerosol particles (Petters and Kreidenweis,  
36 2007).  $\kappa$ -Köhler theory usually performed well in predictions of hygroscopicity and CCN number concentration (Rose et al.,  
37 2010; Kawana et al., 2016; Cai et al., 2020; Zhang et al., 2020). However, remarkable offset was also found because of the  
38 simplifications in  $\kappa$ -Köhler theory (Ruehl et al., 2016; Ovadnevaite et al., 2017). For example, aerosol droplet is assumed to  
39 be diluted near activation and surface tension is usually simply treated as that of pure water, which is sometimes not reasonable  
40 in the presence of atmospheric surfactants (Lowe et al., 2019). Yet many previous studies investigated surface tension effect  
41 of atmospheric surfactant on aerosol CCN activity (Ruehl and Wilson, 2014; Ruehl et al., 2016; Ovadnevaite et al., 2017). At  
42 Mace Head, Ovadnevaite et al. (2017) observed significant underestimation of CCN number concentration (one tenth) in a  
43 nascent ultrafine mode event with high organic mass fraction (55%). The underestimation was improved by applying lower  
44 water surface tension ( $\sim 68\%$  of water surface tension). For surfactant sodium octyl sulfate, Peng et al. (2022) found that CCN-  
45 derived  $\kappa_{\text{CCN}}$  was around 2.4 times larger than growth factor derived  $\kappa_{\text{GF}}$ , which was ascribed to surface tension reduction and  
46 solubility limit. Though established thermodynamic models considering surface tension reductions such as compressed film  
47 model (Ruehl et al., 2016) and liquid-liquid phase separation model (Ovadnevaite et al., 2017; Liu et al., 2018) explained the  
48 discrepancies of CCN activity or CCN number concentration closure, dataset of direct measurement of surface tension for  
49 submicron particles are very rare.

50 Dicarboxylic acids are ubiquitous in atmospheric aerosol particle as a main contributor to organic aerosol mass (mass  
51 contribution to total particulate carbon could exceed 10% in remote area) (Römpf et al., 2006; Ho et al., 2010; Hyder et al.,  
52 2012). Primary emission (e.g. biomass burning and fossil fuel combustion) and secondary formation (e.g. photooxidation of  
53 unsaturated fatty acids) were major sources of dicarboxylic acids (Ho et al., 2010). Furthermore, dicarboxylic acids are also  
54 known as important atmospheric surfactants and their surface activities in water solutions showed a positive relation with  
55 carbon number (Aumann et al., 2010). Currently, most studies investigated surface tension effect of dicarboxylic acids on CCN  
56 activation by measuring surface tension of their solutions and using models based on solution results (Lee and Hildemann,  
57 2013, 2014; Ruehl et al., 2016; Zhang et al., 2021; Vepsäläinen et al., 2022). However, the values derived from bulk solutions  
58 may not be a reasonable represent for aerosol particles because their high surface-to-volume ratio may affect the distribution  
59 of surfactant between surface and bulk (Ruehl et al., 2010; Ruehl and Wilson, 2014). Recently, new methods of surface tension  
60 measurement for particles were introduced such as microfluid (Metcalf et al., 2016) and optical tweezers (Bzdek et al., 2020),  
61 but their samples were micrometre size droplets. Morris et al. (2015) presented a way to directly measure surface tension of  
62 submicron particles under controlled relative humidity (RH) by atomic force microscopy (AFM). Later, AFM was further  
63 reported to be an important tool to probe phase state of individual particles (Lee et al., 2017a; Lee et al., 2017b; Lee and  
64 Tivanski, 2021). However, most measurements using AFM were performed with RH under 95% (Morris et al., 2015; Lee et



65 al., 2017b; Ray et al., 2019; Lee et al., 2020) but rare in higher RH conditions. When RH approaches 100%, Kelvin effect  
66 becomes comparable to the Raoult effect in controlling hygroscopicity, so measurements around 100% RH can help resolve  
67 discrepancies between sub-saturated hygroscopicity and CCN activity (Ruehl and Wilson, 2014).  
68 In this study, we firstly measured CCN activities of internal mixtures containing inorganic salt and dicarboxylic acid. Then,  
69 we directly obtained their surface tension and phase states by AFM under relatively high RH (over 99.5%). Our results could  
70 provide directly dataset of surface tension and phase state of inorganic salts-dicarboxylic acids internal mixed particles, which  
71 would help to decrease the uncertainty for climate models.

## 72 **2 Methods**

### 73 **2.1 Experiments**

#### 74 **2.1.1 Chemicals**

75 Nine used compounds in the present study were sodium chloride (NaCl), ammonium sulfate (AS), malonic acid (MA),  
76 phenylmalonic acid (PhMA), succinic acid (SA), phenylsuccinic acid (PhSA), adipic acid (AA), pimelic acid (PA) and  
77 Octanedioic acid (OA). Their relevant properties investigated in this study were summarized in **Table 1**.

#### 78 **2.1.2 CCN activity measurements**

79 The measurement setup is shown in **Fig. 1**. In brief, particles containing single and mixed chemicals were generated with water  
80 solutions (~ 1%) by a constant output atomizer (TSI 3079A). After drying (RH < 15%), monodispersed aerosol particles were  
81 obtained by differential mobility analyzer (DMA, TSI 3081) with the sheath to sample flow ratio of 10, and then were split  
82 between a condensation particle counter (CPC, TSI 3772) for measuring number concentration of total particles ( $N_{CN}$ ) and a  
83 Cloud Condensation Nuclei Counter (CCNC, DMT-200) for measuring number concentration of CCN ( $N_{CCN}$ ).

84 In this study, the CCNC was operated in Scanning Flow CCN Analysis (SFCA) mode, which was introduced elsewhere (Moore  
85 and Nenes, 2009). In short, the pressure and  $\Delta T$  of CCNC were kept constant, the flow rate was continuously and linearly  
86 varied from 0.2 L min<sup>-1</sup> to 1 L min<sup>-1</sup> or vice versa (1-0.2 L min<sup>-1</sup>) within 125 s and the interval time for stabilization is 25 s.  
87 The supersaturations in CCNC was calibrated under four  $\Delta T$  (4K, 6K, 10K and 18K). We obtained sigmoidal curves of  
88 activation ratio ( $N_{CCN}/N_{CN}$ ) versus flow rate, then fitted the inflection point of the curves as critical flow rate  $Q_{50}$ . Ammonium  
89 sulfate was used to determine supersaturation ratio with an activity parameterization Köhler model AP3 as suggested by Rose  
90 et al. (2008). The calibration results were showed in **Fig. S1**.

#### 91 **2.1.3 Surface tension measurements**

92 As showed in **Fig.1**, samples for AFM analysis were collected through deposition by impaction with an eight stage non-viable  
93 particle sizing sampler (Models BGI20800 Series, BGI Incorporation) onto hydrophobically silicon wafers (Ding et al., 2020).



94 The aerodynamic size of collected particles was ranged in 0.4  $\mu\text{m}$ -1  $\mu\text{m}$  (50% efficiency). The substrate deposited particles  
95 were stored under dry condition (RH < 10%) and most of the samples were studied at the same day to avoid possible sample  
96 aging.

97 Surface tension measurement was performed using an AFM system (Cypher ES, Asylum Research). Cypher ES contains a  
98 small cell with air inlet and outlet, it enables to scan samples under different environmental conditions such as RH. RH in cell  
99 was achieved and maintained by humidified flow. RH in cell was measured by a RH sensor (SHT 85, Sensirion Inc.). Custom-  
100 built high aspect ratio (HAR) platinum AFM probes with constant diameter and nominal spring constant of  $\sim 3.0 \text{ N m}^{-1}$  were  
101 used for particle imaging and surface tension measurements (**Fig. S2**) (Morris et al., 2015). The platinum nanoneedles could  
102 well measure surface tension of pure water and 1, 3-propanediol (**Fig. S3**). The procedures of making nanotips were detailly  
103 described in a manuscript under review and a brief description was given here. Firstly, dual-beam-focused ion beam (FIB,  
104 ZEISS crossbeam 350) microscope was used to etch the top of the tip (Multi75Al-G purchased from BudgetSensors Inc.),  
105 making the etched tip flat. Then, FIB was used to deposit a cylindrical metal platinum column (100 nm-500 nm diameter) on  
106 the flat surface of the etched tip.

107 The principles of surface tension measurement using AFM were described elsewhere (Yazdanpanah et al., 2008; Morris et al.,  
108 2015; Lee et al., 2017a). Collected samples were firstly imaged in tapping mode to locate individual particles under dry  
109 condition (RH < 10%), then the RH gradually increased to over 99.5% in  $\sim 40$  minutes (**Fig.S4**). Force-distance plots of droplet  
110 were obtained by contact mode. A tip velocity of 1-2  $\mu\text{m s}^{-1}$  and dwell time of 1-2 seconds were used for all measurements  
111 (Kaluarachchi et al., 2021). More than 10 force plots were collected on at least 5 individual droplets. Precise diameter of  
112 nanoneedle was calibrated by measuring surface tension of pure water by adding a water droplet (2-3 mm height) onto silicon  
113 wafer (Kaluarachchi et al., 2021). New probe was used for different chemicals in order to avoid possible contamination of the  
114 AFM probe.

## 115 2.2 Theory

116 Based on  $\kappa$ -Köhler theory, hygroscopicity parameter  $\kappa_{\text{CCN}}$  can be calculated by:

$$117 \kappa_{\text{CCN}} = \frac{4A^3}{27D_d^3 \ln^2(1+s_c)}, A = \frac{4M_w \sigma_w}{RT \rho_w} \quad (1)$$

118 where  $\sigma_w$ ,  $M_w$  and  $\rho_w$  are surface tension, molecular weight and density of water, respectively.  $R$  is universal gas constant and  
119  $T$  is temperature (298.15K).  $s_c$  is critical supersaturation ratio.  $D_d$  is dry diameter. In addition, hygroscopicity  $\kappa$  of  
120 multicomponent chemical system can also be calculated assuming a Zdanovskii, Stokes, and Robinson (ZSR) simple mixing  
121 rule.  $\kappa$  based on the chemical composition ( $\kappa_{\text{Chem}}$ ) of mixed aerosol was calculated by:

$$122 \kappa_{\text{Chem}} = OVF \cdot \kappa_{\text{org}} + (1 - OVF) \cdot \kappa_{\text{inorg}}, \quad (2)$$



123 where  $\kappa_{\text{org}}$  and  $\kappa_{\text{inorg}}$  are hygroscopicity  $\kappa$  values (here obtained  $\kappa_{\text{CCN}}$  values were used) of single organic acids and inorganic  
124 salts.

125 As described by Morris et al. (2015), the basis of surface tension measurement for a liquid droplet by AFM was calculated by:

$$126 \quad \sigma = \frac{F_r}{2\pi r}, \quad (3)$$

127 where  $F_r$  is the retention force to break the meniscus by the tip of AFM probe,  $r$  is the radius of the AFM probe tip, and  $\sigma$  is  
128 surface tension of the droplet. The retention force is the force difference before and after the probe was just retracted from the  
129 droplet.

### 130 3 Results and discussion

#### 131 3.1 $\kappa_{\text{CCN}}$ of single component

132  $\kappa_{\text{CCN}}$  values for single component aerosols were summarized in **Table 2**.  $\kappa_{\text{CCN}}$  of NaCl, AS, MA, SA and AA were  $1.325 \pm$   
133  $0.038$ ,  $0.562 \pm 0.059$ ,  $0.240 \pm 0.036$ ,  $0.204 \pm 0.023$  and  $0.008 \pm 0.001$ , respectively, being consistent with previous results  
134 (Petters and Kreidenweis, 2007; Kuwata et al., 2013).  $\kappa_{\text{CCN}}$  of PA and OA were  $0.112 \pm 0.010$  and  $0.003 \pm 0.0002$ , which were  
135 20% lower and twice higher than those reported by Kuwata et al. (2013). Possible factor may be the purity of solutes, because  
136 additional hydrophobic (or hygroscopic) matters in commercial reagents may possibly decrease (increase) organic  
137 hygroscopicity (Hings et al., 2008).  $\kappa_{\text{CCN}}$  values of PhMA and PhSA were  $0.183 \pm 0.032$  and  $0.145 \pm 0.017$ , respectively,  
138 which to our knowledge are firstly reported in this study.

139 Solubility and molar volume of dicarboxylic acids were essential factors influencing their hygroscopicity (Kumar et al., 2003;  
140 Han et al., 2022). In this study, we considered two regimes: highly soluble organic components (with water solubility over 100  
141  $\text{g L}^{-1}$ ) and slightly soluble organic components (with water solubility between 10-100  $\text{g L}^{-1}$ ), which was consistent with  
142 previous study (Kuwata et al., 2013). As showed in **Fig. 2a**, the  $\kappa_{\text{CCN}}$  values for highly soluble components decreased linearly  
143 with increased molecular volumes. This trend was similar to  $\kappa_{\text{CCN}}$  values for sugar as well as dicarboxylic acids reported by  
144 Chan et al. (2008). In **Fig. 2b**,  $\kappa_{\text{CCN}}$  values of sparsely soluble components (AA, PA, SA and OA) showed an increased trend  
145 with solubility, as organic matter with the higher water solubility would dissolve more and have a higher molar concentration,  
146 resulting in reduction in water activity and higher hygroscopicity (Luo et al., 2020; Han et al., 2022).

147 Organic functional group could also affect hygroscopicity (Suda et al., 2014; Petters et al., 2017).  $\kappa_{\text{CCN}}$  of PA (0.112) was  
148 higher than those of AA (0.008) and OA (0.003), which is contrary to results in Suda et al. (2014) and Petters et al. (2017) that  
149 hygroscopicity decreased with increased number of methylene. This phenomenon was attributed to the odd-even effect of  
150 dicarboxylic acids, that is, diacids with odd numbers of carbon atoms being more soluble than those with adjacent even  
151 numbers (Zhang et al., 2013). Furthermore,  $\kappa_{\text{CCN}}$  values of PhMA and PhSA were both lower than that of MA and SA,  
152 respectively, indicating that the addition of phenyl showed negative effects on hygroscopicity. The addition of phenyl



153 substitution increased the molar volumes of MA and SA and may contribute to the drops of hygroscopicity (Petters et al.,  
154 2009).

### 155 3.2 $\kappa_{\text{CCN}}$ of inorganic salt-dicarboxylic acid mixed components

156 **Figure 3** presents the  $\kappa_{\text{CCN}}$  values of inorganic salt/dicarboxylic acid mixed particles with varied organic volume fractions  
157 (OVF). Overall,  $\kappa_{\text{CCN}}$  of each inorganic salt/dicarboxylic acid system showed a decreased trend with increased OVF. For  
158 example,  $\kappa_{\text{CCN}}$  of AS/MA particles with OVF of 57%, 73% and 88% were 0.399, 0.373 and 0.336, respectively. Larger fractions  
159 of dicarboxylic acids (with low hygroscopicity compares to inorganic salts) caused more decrease in hygroscopicity of  
160 inorganic/dicarboxylic acid system. As for inorganic salt/dicarboxylic acid systems with same OVF,  $\kappa_{\text{CCN}}$  values of systems  
161 of AS/MA, AS/SA, AS/PhMA, AS/PhSA and AS/PA with 57% OVF were 0.399, 0.382, 0.364, 0.340 and 0.334, following  
162 the order of  $\kappa_{\text{CCN}}$  values of single dicarboxylic acid (**Fig. 3a**). However,  $\kappa_{\text{CCN}}$  values of NaCl/AA and NaCl/OA mixed particles  
163 with OVF of 60% were 0.734 and 0.685, even higher than that of NaCl/MA (0.639), demonstrating an opposite trend with  
164 respect to those of single components. This discrepancy could be ascribed to surface tension reduction because AA and OA  
165 showed different physical properties (e.g. deliquescence point, surface activity and solubility) when comparing with the other  
166 organics, thus may result in distinct microphysics processes during interactions with inorganic salts and water content. AA and  
167 OA own lowest solubilities and high deliquescence RH (**Table 1**) among experimental dicarboxylic acids, which potentially  
168 lead to their weak CCN activities (Hings et al., 2008). However, inorganic salts were found to facilitate the deliquescence of  
169 dicarboxylic acid (Bilde and Svenningsson, 2004; Sjogren et al., 2007; Minambres et al., 2013). AS/AA mixed particles  
170 deliquescence under 78%-83% RH with mass fractions of AA between 50%-80% (Sjogren et al., 2007). Small amount of NaCl  
171 (2% mass fraction) could notably decrease  $s_c$  of AA with 80 nm dry diameter from over 2% to ~0.6% (Bilde and Svenningsson,  
172 2004). Thus, addition of inorganic salts facilitates deliquescence of OA and AA under lower RH, which may further promote  
173 phase state transition from solid to liquid (or semisolid) and cause surface tension reductions as OA and AA show stronger  
174 surface activities than most of the rest dicarboxylic acids because of longer carbon chain (Aumann et al., 2010). This indication  
175 was further confirmed by AFM surface tension measurement, as discussed in Section 3.4.

### 176 3.3 Closure study between $\kappa_{\text{CCN}}$ and $\kappa_{\text{Chem}}$

177  $\kappa_{\text{CCN}}$  and  $\kappa_{\text{Chem}}$  values for inorganic salt/dicarboxylic acid mixed particles were showed in **Fig. 4**.  $\kappa_{\text{CCN}}$  values of inorganic salt  
178 and most dicarboxylic acids (MA, PhMA, SA, PhSA and PA) mixed particles could be predicted by ZSR mixing rule with  
179 relative difference below 30% (**Fig. 4a**). Similar results have been found in previous lab and filed studies (Ruehl et al., 2012;  
180 Kuwata et al., 2013; Wu et al., 2013; Dawson et al., 2016; Nguyen et al., 2017; Ovadnevaite et al., 2017), indicating that semi-  
181 experimental ZSR mixing rule could be a useful method to predicted mixed particles hygroscopicity and CCN activation. For  
182 instance, Dawson et al. (2016) reported consistence between  $\kappa_{\text{CCN}}$  and  $\kappa_{\text{Chem}}$  for NaCl/xanthan gum and CaCO<sub>3</sub>/xanthan gum  
183 mixed particles within 10% uncertainty. Wu et al. (2013) also obtained same closure results in a field study at central Germany,





184 for particles containing 60%-80% organic mass fraction and 30%-50% inorganic salts. Meanwhile, CCN studies also found  
185 that using  $\kappa_{\text{Chem}}$  could well predict measured CCN number concentration (Juranyi et al., 2010; Rose et al., 2010; Almeida et  
186 al., 2014; Kawana et al., 2016; Cai et al., 2020; Zhang et al., 2020). However, for inorganic/AA and inorganic/OA mixed  
187 particles (**Fig. 4b**), their  $\kappa_{\text{CCN}}$  values were 0.3-3.0 times higher than  $\kappa_{\text{Chem}}$ . Surface tension reduction was one of the potential  
188 causes, as discussed in section 3.2 that OA and AA with strong surface activity and low solubilities may result in stronger  
189 surface tension reduction than most of the rest dicarboxylic acids. In addition, the underprediction showed a gradual increased  
190 trend with increased OVF since increased OVF lead to higher concentration of organics, thus leading to more surface tension  
191 reduction. Surface tension reduction in water solution caused by atmospheric surfactants were observed frequently in previous  
192 studies (Facchini et al., 1999; Gerard et al., 2016). Results have showed that neglect of surface tension reduction may lead to  
193 higher  $\kappa_{\text{CCN}}$  values than  $\kappa_{\text{Chem}}$  or growth factor derived  $\kappa_{\text{GF}}$  (Irwin et al., 2010; Wu et al., 2013; Zhao et al., 2016; Hu et al.,  
194 2020; Peng et al., 2021), as well as underpredictions of CCN number concentration (Good et al., 2010; Asa-Awuku et al., 2011;  
195 Ovadnevaite et al., 2017; Cai et al., 2020). Hu et al. (2020) reported that  $\kappa_{\text{Chem}}$  underpredicted  $\kappa_{\text{CCN}}$  by 13% and 18% at  
196 supersaturation ratios of 0.1% and 0.3%, which may be attributed to the depression of droplet surface tension by potential  
197 surface-active organics. Likewise, Ovadnevaite et al. (2017) only predicted one tenth of measured CCN number concentration  
198 in a nascent ultrafine mode event because of the surface tension reduction, and the notable underestimation was improved by  
199 applying lower water surface tension ( $\sim 68\%$  of water surface tension) in  $\kappa$ -Köhler theory.

200 Apart from surface tension reduction, aerosol phase states could also bring uncertainty to critical supersaturation and  
201 hygroscopicity predictions (Henning et al., 2005; Hodas et al., 2015; Peng et al., 2016; Zhao et al., 2016). Being different from  
202 tradition Köhler curve with only one maximum, modified Köhler curve for inorganic salt and slightly soluble dicarboxylic  
203 acid (e.g. AA) mixed particles accounting for limited solubility obtained two maxima of critical supersaturation ratios and the  
204 higher value among the two maxima determined CCN activation (Bilde and Svenningsson, 2004). The maximum at the larger  
205 wet diameter is identical with that obtained by assuming that the organic acids are infinitely soluble in water (i.e. classical  
206 Köhler theory). And the other maximum with smaller wet diameter represents the point that all slightly soluble material is  
207 fully dissolved and the maximum can also be viewed as an activation barrier which is due to the presence of a undissolved  
208 solid part of organic acid (Henning et al., 2005). Pajunoja et al. (2015) reported that biogenic secondary organic aerosol (SOA)  
209 particles formed from isoprene showed an increased trend of hygroscopicity parameter from 0.05 to nearly 0.15 when RH  
210 increased from 40% to supersaturation. They indirectly found the biogenic SOA to be semisolid phase thus the increased trend  
211 of hygroscopicity  $\kappa$  was explained by the gradual phase transition from solid to semisolid (or liquid) with raised RH because  
212 water content may gradually wet and dissolve the organic surface and form water film (Pajunoja et al., 2015). The phase  
213 transition (or water film formation) of pure OA and AA would be difficult (i.e. high RH is required) because of their high  
214 deliquescence point and low solubilities, but could be easier (i.e. required high RH is decreased) by addition of inorganic salts.

215 Overall, phase state and surface tension of atmospheric aerosol were two essential factors influencing their hygroscopicity and



216 CCN activation. Though there are several indirect ways detecting aerosol phase state (Pajunoja et al., 2015; Shiraiwa et al.,  
217 2017), current studies about directly measurements are still very limited.

### 218 **3.4 Phase state and surface tension of inorganic salt/dicarboxylic acid mixed particles**

#### 219 **3.4.1 Phase state**

220 We obtained phase states of inorganic salt/dicarboxylic acid under high RH environment (over 99.5%) by analyzing shapes of  
221 force plot based on AFM system (Lee et al., 2017a; Lee and Tivanski, 2021). **Figure 5a** showed force plot of NaCl/MA mixed  
222 particles with 75% OVF. AFM probe needle tip approached the droplet vertically before contacting with droplet, needle tip  
223 was not disturbed by extra force (red line). Then, needle tip came in contact with the droplet, resulting in an abrupt negative  
224 force (i.e. needle was attracting by drop). After that, needle moved through the droplet with negative force until contacting  
225 with the substrate. When tip contacted substrate, the negative force would quickly be positive (repulsive force), exceeding a  
226 predefined maximum amount of force. Then the tip retracted back away from the droplet, as indicates by blue line. Because  
227 of the surface tension of droplet surface, needle tip would experience attractive force and abruptly turned to zero when tip  
228 separated from droplet surface. Our observation in **Fig. 5a** showed a similar shape with results reported by Morris et al. (2015),  
229 indicating the particles were liquid. Most of the studied inorganic salt/dicarboxylic acid (MA, PhMA, SA, PhSA and PA) were  
230 liquid under RH over 99.5%.

231 However, for AS/SA (72% and 88% OVF), NaCl/AA (89% OVF), AS/AA (57%, 72% and 88% OVF) and AS/OA (88%  
232 OVF), the shape force plots were totally different. During the tip contacting with particle, force plots showing a jaggging profile,  
233 as shown in **Fig. 5b**. This shape is nearly the same as the curves for NaBr particles under 52% RH reported by Lee et al.  
234 (2017a). They explained the phase of NaBr was semi-solid and jaggging profile in tip approaching was caused by its viscosity.  
235 Therefore, AS/SA (72% and 88% OVF), NaCl/AA (89% OVF), AS/AA (57%, 72% and 88% OVF) and AS/OA (88% OVF)  
236 mixed particles were indicated to be semisolid. Semisolid phase states were more likely to occur when containing higher OVF  
237 of dicarboxylic acids with lower solubilities and higher deliquescence point (SA, AA and OA) and inorganic salts with  
238 comparative lower hygroscopicity (AS), as in this circumstance water content may be insufficient and could not easily dissolve  
239 organics. Therefore, semisolid phase of inorganic salt/AA and inorganic salt/OA mixed particles provides evident for phase  
240 state effect on aerosol hygroscopicity, which may attribute to higher  $\kappa_{CCN}$  than  $\kappa_{Chem}$  as discussed in section 3.3 (**Fig 4b**).  
241 Though AS/SA mixed particles (72% and 88% OVF) were semisolid because of high deliquescence point (98%) of SA, their  
242 good closure between  $\kappa_{CCN}$  and  $\kappa_{Chem}$  may ascribe to higher solubility of SA, which may intensify the water absorption after  
243 deliquescence thus phase transition from semisolid to diluted liquid when activating to CCN.

#### 244 **3.4.2 Surface tension**

245 Lee et al. (2017a) pointed out that surface tension calculation could not be achieved for semisolid particles, because the  
246 measured retention force was not solely attributed to surface tension, but have additional contributions that include viscosity.





247 Therefore, only surface tensions of inorganic salt/dicarboxylic acid mixed particles that were liquid were further obtained by  
248 **Eq.3**. Surface tension results were summarized in **Fig. 6**. Overall, surface tensions of all inorganic salt/dicarboxylic acid mixed  
249 particles showed a decrease trend with increased OVF as higher OVF may result in higher organic solute concentrations thus  
250 caused more surface tension reduction. Surface tensions of inorganic salts mixed with MA, PhMA, SA, PhSA and PA lowered  
251 by within 12% than that of pure water ( $72 \text{ mN m}^{-1}$ ), indicating that droplets got strongly diluted at RH over 99.5%, and ought  
252 to be more diluted when activation occurs. This may contribute to  $\kappa$  closure within 30% deviation in **Fig. 4a** because diluted  
253 solution and water surface tension were assumed in  $\kappa$ -Köhler theory. However, surface tensions of inorganic salts/AA and  
254 inorganic salts/OA mixed particles showed notable reductions (20%-42%), which may contribute to their higher  $\kappa_{\text{CCN}}$  values  
255 than  $\kappa_{\text{Chem}}$  (**Fig. 4b**). Besides, notable surface tension reductions of particles containing OA or AA indicated that organic  
256 solubility plays an important role in surface tension reduction as AA and OA have the lowest solubilities among studied  
257 dicarboxylic acids. Besides, OA and AA own higher deliquescence point and longer carbon chains than most of the rest studied  
258 organics and thus deliquescence RH and strong surface activity are also essential factors attributing to surface tension reduction  
259 for inorganic salt/dicarboxylic acid mixed particles. Furthermore, for dicarboxylic acids, lower organic solubilities may be  
260 more important factor causing surface tension reduction than deliquescence RH and surface activity. This was because PA  
261 with higher solubility, but similar deliquescence RH and surface activity like AA and OA did not show much depression of  
262 surface tension when mixed with inorganic salts.

#### 263 4 Conclusions

264 The role of surfactants such as dicarboxylic acids in CCN activity were often ignored in aerosol hygroscopicity studies and  
265 currently climate models. In this study, we analyzed CCN activities of inorganic salt/dicarboxylic acid internal mixed particles  
266 with varied OVF and directly measured their phase state and surface tension by AFM under relative high RH.

267  $\kappa_{\text{CCN}}$  values of single dicarboxylic acid located in the range of 0.003-0.240. A linearly positive relation between  $\kappa_{\text{CCN}}$  and  
268 solubility were obtained for slightly dissolved species, while negative relation was found between  $\kappa_{\text{CCN}}$  and molecular volume  
269 for highly soluble species.  $\kappa_{\text{CCN}}$  of PhMA and PhSA were lower than those of MA and SA, respectively, revealing that addition  
270 of phenyl radical could weaken hygroscopicity of dicarboxylic acid.

271 For most inorganic salt/dicarboxylic acid (MA, PhMA, SA, PhSA and PA),  $\kappa_{\text{CCN}}$  of mixed particles with same OVF showed  
272 an overall decrease trend and followed the order of  $\kappa_{\text{CCN}}$  values of single dicarboxylic acid. Good closure within 30% relative  
273 bias between  $\kappa_{\text{CCN}}$  and  $\kappa_{\text{Chem}}$  were obtained. On the contrast, our results demonstrated that the semisolid phase state and surface  
274 tension reduction (20%-42%) are the potential factors to explain the enhanced CCN activity of inorganic salts/OA and  
275 inorganic salts/AA mixed particles. Slightly dissolved dicarboxylic acids with lower solubilities, higher deliquescence point  
276 and surface activity are more likely to cause notable surface tension depression for inorganic salt/dicarboxylic acid mix  
277 particles. Therefore, we proposed that surface tension reduction and phase state should be carefully considered in future models



278 and observations, especially for slightly soluble organics with lower solubilities, high deliquescence RH and strong surface  
279 activity.

280

281 **Data availability.** The data used in this paper can be obtained from the corresponding author upon request.

282 **Author contributions.** CX did the experiments, analyzed data, plotted the figures and wrote the original draft. BYK contributed  
283 data analyzing and discussion, reviewed the manuscript and contributed to fund acquisition. XLD and XYP contributed to the  
284 instrumentation and discussion. ZNX contributed to the discussion and fund acquisition. HH contributed to the instrumentation,  
285 discussion and fund acquisition. ZBW administrated the project, conceptualized the study, reviewed the manuscript and  
286 contributed to fund acquisition.

287 **Acknowledgment.** The research was supported by National Natural Science Foundation of China (91844301, 42005087,  
288 61974128 and 42005086) and the Fundamental Research Funds for the Central Universities (2018QNA6008). We appreciate  
289 Shikuan Yang, Qianqian Ding and Xueyan Chen for making and kindly sharing hydrophobically silicon wafers. We likewise  
290 thank Ren Zhu, Lin Liu, Renwei Mao and Yuzhong Zhang for the discussions about AFM experiment.

291 **Competing interests.** The authors declare no competing financial interest.

## 292 **References**

293 Almeida, G. P., Brito, J., Morales, C. A., Andrade, M. F., and Artaxo, P.: Measured and modelled cloud condensation nuclei  
294 (CCN) concentration in Sao Paulo, Brazil: the importance of aerosol size-resolved chemical composition on CCN  
295 concentration prediction, *Atmos. Chem. Phys.*, 14, 7559-7572, <https://doi.org/10.5194/acp-14-7559-2014>, 2014.

296 Asa-Awuku, A., Moore, R. H., Nenes, A., Bahreini, R., Holloway, J. S., Brock, C. A., Middlebrook, A. M., Ryerson, T. B.,  
297 Jimenez, J. L., DeCarlo, P. F., Hecobian, A., Weber, R. J., Stickel, R., Tanner, D. J., and Huey, L. G.: Airborne cloud  
298 condensation nuclei measurements during the 2006 Texas Air Quality Study, *J. Geophys. Res.: Atmos.*, 116, D11201,  
299 <https://doi.org/10.1029/2010jd014874>, 2011.

300 Aumann, E., Hildemann, L. M., and Tabazadeh, A.: Measuring and modeling the composition and temperature-dependence of  
301 surface tension for organic solutions, *Atmos. Environ.*, 44, 329-337, <https://doi.org/10.1016/j.atmosenv.2009.10.033>, 2010.

302 Bilde, M. and Svenningsson, B.: CCN activation of slightly soluble organics: the importance of small amounts of inorganic  
303 salt and particle phase, *Tellus B: Chem. Phys. Meteorol.*, 56, 128-134, <https://doi.org/10.3402/tellusb.v56i2.16406>, 2004.

304 Bzdek, B. R., Reid, J. P., Malila, J., and Prisle, N. L.: The surface tension of surfactant-containing, finite volume droplets,  
305 *Proc. Natl. Acad. Sci. U.S.A.*, 117, 8335-8343, <https://doi.org/10.1073/pnas.1915660117>, 2020.

306 Cai, M., Liang, B., Sun, Q., Zhou, S., Chen, X., Yuan, B., Shao, M., Tan, H., and Zhao, J.: Effects of continental emissions on  
307 cloud condensation nuclei (CCN) activity in the northern South China Sea during summertime 2018, *Atmos. Chem. Phys.*, 20,  
308 9153-9167, <https://doi.org/10.5194/acp-20-9153-2020>, 2020.



- 309 Chan, M. N., Kreidenweis, S. M., and Chan, C. K.: Measurements of the hygroscopic and deliquescence properties of organic  
310 compounds of different solubilities in water and their relationship with cloud condensation nuclei activities, *Environ. Sci.*  
311 *Technol.*, 42, 3602-3608, <https://doi.org/10.1021/es7023252>, 2008.
- 312 Dawson, K. W., Petters, M. D., Meskhidze, N., Petters, S. S., and Kreidenweis, S. M.: Hygroscopic growth and cloud droplet  
313 activation of xanthan gum as a proxy for marine hydrogels, *J. Geophys. Res.: Atmos.*, 121, 11803–11818,  
314 <https://doi.org/10.1002/2016jd025143>, 2016.
- 315 Ding, Q., Wang, J., Chen, X., Liu, H., Li, Q., Wang, Y., and Yang, S.: Quantitative and sensitive SERS platform with analyte  
316 enrichment and filtration function, *Nano Lett.*, 20, 7304-7312, <https://doi.org/10.1021/acs.nanolett.0c02683>, 2020.
- 317 Dusek, U., Frank, G. P., Hildebrandt, L., Curtius, J., Schneider, J., Walter, S., Chand, D., Drewnick, F., Hings, S., Jung, D.,  
318 Borrmann, S., and Andreae, M. O.: Size matters more than chemistry for cloud-nucleating ability of aerosol particles, *Science*,  
319 312, 1375-1378, <https://doi.org/10.1126/science.1125261>, 2006.
- 320 Facchini, M. C., Mircea, M., Fuzzi, S., and Charlson, R. J.: Cloud albedo enhancement by surface-active organic solutes in  
321 growing droplets, *Nature*, 401, 257-259, <https://doi.org/10.1038/45758>, 1999.
- 322 Gerard, V., Noziere, B., Baduel, C., Fine, L., Frossard, A. A., and Cohen, R. C.: Anionic, Cationic, and Nonionic Surfactants  
323 in Atmospheric Aerosols from the Baltic Coast at Asko, Sweden: Implications for Cloud Droplet Activation, *Environ Sci*  
324 *Technol*, 50, 2974-2982, <https://doi.org/10.1021/acs.est.5b05809>, 2016.
- 325 Good, N., Topping, D. O., Allan, J. D., Flynn, M., Fuentes, E., Irwin, M., Williams, P. I., Coe, H., and McFiggans, G.:  
326 Consistency between parameterisations of aerosol hygroscopicity and CCN activity during the RHaMBLe discovery cruise,  
327 *Atmos. Chem. Phys.*, 10, 3189-3203, <https://doi.org/10.5194/acp-10-3189-2010>, 2010.
- 328 Gunthe, S. S., King, S. M., Rose, D., Chen, Q., Roldin, P., Farmer, D. K., Jimenez, J. L., Artaxo, P., Andreae, M. O., Martin,  
329 S. T., and Pöschl, U.: Cloud condensation nuclei in pristine tropical rainforest air of Amazonia: size-resolved measurements  
330 and modeling of atmospheric aerosol composition and CCN activity, *Atmos. Chem. Phys.*, 9, 7551-7575,  
331 <https://doi.org/10.5194/acp-9-7551-2009>, 2009.
- 332 Han, S., Hong, J., Luo, Q., Xu, H., Tan, H., Wang, Q., Tao, J., Zhou, Y., Peng, L., He, Y., Shi, J., Ma, N., Cheng, Y., and Su,  
333 H.: Hygroscopicity of organic compounds as a function of organic functionality, water solubility, molecular weight, and  
334 oxidation level, *Atmos. Chem. Phys.*, 22, 3985-4004, <https://doi.org/10.5194/acp-22-3985-2022>, 2022.
- 335 Henning, S., Rosenorn, T., D'Anna, B., Gola, A. A., Svenningsson, B., and Bilde, M.: Cloud droplet activation and surface  
336 tension of mixtures of slightly soluble organics and inorganic salt, *Atmos. Chem. Phys.*, 5, 575-582,  
337 <https://doi.org/10.5194/acp-5-575-2005>, 2005.
- 338 Hings, S. S., Wrobel, W. C., Cross, E. S., Worsnop, D. R., Davidovits, P., and Onasch, T. B.: CCN activation experiments  
339 with adipic acid: effect of particle phase and adipic acid coatings on soluble and insoluble particles, *Atmos. Chem. Phys.*, 8,  
340 3735-3748, <https://doi.org/10.5194/acp-8-3735-2008>, 2008.
- 341 Ho, K. F., Lee, S. C., Ho, S. S. H., Kawamura, K., Tachibana, E., Cheng, Y., and Zhu, T.: Dicarboxylic acids, ketocarboxylic  
342 acids,  $\alpha$ -dicarbonyls, fatty acids, and benzoic acid in urban aerosols collected during the 2006 Campaign of Air Quality



- 343 Research in Beijing (CAREBeijing-2006), *J. Geophys. Res.: Atmos.*, 115, D19312, <https://doi.org/10.1029/2009jd013304>,  
344 2010.
- 345 Hodas, N., Zuend, A., Mui, W., Flagan, R. C., and Seinfeld, J. H.: Influence of particle-phase state on the hygroscopic behavior  
346 of mixed organic–inorganic aerosols, *Atmos. Chem. Phys.*, 15, 5027–5045, <https://doi.org/10.5194/acp-15-5027-2015>, 2015.
- 347 Hu, D., Liu, D., Zhao, D., Yu, C., Liu, Q., Tian, P., Bi, K., Ding, S., Hu, K., Wang, F., Wu, Y., Wu, Y., Kong, S., Zhou, W.,  
348 He, H., Huang, M., and Ding, D.: Closure investigation on cloud condensation nuclei ability of processed anthropogenic  
349 aerosols, *J. Geophys. Res.: Atmos.*, 125, e2020JD032680, <https://doi.org/10.1029/2020jd032680>, 2020.
- 350 Hyder, M., Genberg, J., Sandahl, M., Swietlicki, E., and Jönsson, J. Å.: Yearly trend of dicarboxylic acids in organic aerosols  
351 from south of Sweden and source attribution, *Atmos. Environ.*, 57, 197–204, <https://doi.org/10.1016/j.atmosenv.2012.04.027>,  
352 2012.
- 353 Irwin, M., Good, N., Crosier, J., Choularton, T. W., and McFiggans, G.: Reconciliation of measurements of hygroscopic  
354 growth and critical supersaturation of aerosol particles in central Germany, *Atmos. Chem. Phys.*, 10, 11737–11752,  
355 <https://doi.org/10.5194/acp-10-11737-2010>, 2010.
- 356 Juranyi, Z., Gysel, M., Weingartner, E., DeCarlo, P. F., Kammermann, L., and Baltensperger, U.: Measured and modelled  
357 cloud condensation nuclei number concentration at the high alpine site Jungfraujoch, *Atmos. Chem. Phys.*, 10, 7891–7906,  
358 <https://doi.org/10.5194/acp-10-7891-2010>, 2010.
- 359 Kaluarachchi, C. P., Lee, H. D., Lan, Y., Lansakara, T. I., and Tivanski, A. V.: Surface tension measurements of aqueous  
360 liquid–air interfaces probed with microscopic indentation, *Langmuir*, 37, 2457–2465,  
361 <https://doi.org/10.1021/acs.langmuir.0c03507>, 2021.
- 362 Kawana, K., Nakayama, T., and Mochida, M.: Hygroscopicity and CCN activity of atmospheric aerosol particles and their  
363 relation to organics: Characteristics of urban aerosols in Nagoya, Japan, *J. Geophys. Res.: Atmos.*, 121, 4100–4121,  
364 <https://doi.org/10.1002/2015jd023213>, 2016.
- 365 Köhler, H.: The nucleus in and the growth of hygroscopic droplets, *Trans. Faraday Soc.*, 32, 1152–1161,  
366 <https://doi.org/10.1039/tf9363201152>, 1936.
- 367 Kumar, P. P., Broekhuizen, K., and Abbatt, J. P. D.: Organic acids as cloud condensation nuclei: Laboratory studies of highly  
368 soluble and insoluble species, *Atmos. Chem. Phys.*, 3, 509–520, <https://doi.org/10.5194/acp-3-509-2003>, 2003.
- 369 Kuwata, M., Shao, W., Lebouteiller, R., and Martin, S. T.: Classifying organic materials by oxygen-to-carbon elemental ratio  
370 to predict the activation regime of Cloud Condensation Nuclei (CCN), *Atmos. Chem. Phys.*, 13, 5309–5324,  
371 <https://doi.org/10.5194/acp-13-5309-2013>, 2013.
- 372 Lee, H. D., Estillore, A. D., Morris, H. S., Ray, K. K., Alejandro, A., Grassian, V. H., and Tivanski, A. V.: Direct surface  
373 tension measurements of individual sub-micrometer particles using atomic force microscopy, *J. Phys. Chem. A*, 121, 8296–  
374 8305, <https://doi.org/10.1021/acs.jpca.7b04041>, 2017a.



- 375 Lee, H. D., Ray, K. K., and Tivanski, A. V.: Solid, semisolid, and liquid phase states of individual submicrometer particles  
376 directly probed using atomic force microscopy, *Anal. Chem.*, 89, 12720-12726, <https://doi.org/10.1021/acs.analchem.7b02755>,  
377 2017b.
- 378 Lee, H. D., Morris, H. S., Laskina, O., Sultana, C. M., Lee, C., Jayarathne, T., Cox, J. L., Wang, X., Hasenecz, E. S., DeMott,  
379 P. J., Bertram, T. H., Cappa, C. D., Stone, E. A., Prather, K. A., Grassian, V. H., and Tivanski, A. V.: Organic enrichment,  
380 physical phase state, and surface tension depression of nascent core-shell sea spray aerosols during two phytoplankton blooms,  
381 *ACS Earth Space Chem.*, 4, 650-660, <https://doi.org/10.1021/acsearthspacechem.0c00032>, 2020.
- 382 Lee, H. D. and Tivanski, A. V.: Atomic force microscopy: An emerging tool in measuring the phase state and surface tension  
383 of individual aerosol particles, *Annu. Rev. Phys. Chem.*, 72, 235-252, <https://doi.org/10.1146/annurev-physchem-090419->  
384 110133, 2021.
- 385 Lee, J. Y. and Hildemann, L. M.: Surface tension of solutions containing dicarboxylic acids with ammonium sulfate, d-glucose,  
386 or humic acid, *J. Aerosol Sci.*, 64, 94-102, <https://doi.org/10.1016/j.jaerosci.2013.06.004>, 2013.
- 387 Lee, J. Y. and Hildemann, L. M.: Surface tensions of solutions containing dicarboxylic acid mixtures, *Atmos. Environ.*, 89,  
388 260-267, <https://doi.org/10.1016/j.atmosenv.2014.02.049>, 2014.
- 389 Liu, P. F., Song, M. J., Zhao, T. N., Gunthe, S. S., Ham, S. H., He, Y. P., Qin, Y. M., Gong, Z. H., Amorim, J. C., Bertram, A.  
390 K., and Martin, S. T.: Resolving the mechanisms of hygroscopic growth and cloud condensation nuclei activity for organic  
391 particulate matter, *Nat. Commun.*, 9, 4076, <https://doi.org/10.1038/s41467-018-06622-2>, 2018.
- 392 Lowe, S. J., Partridge, D. G., Davies, J. F., Wilson, K. R., Topping, D., and Riipinen, I.: Key drivers of cloud response to  
393 surface-active organics, *Nat. Commun.*, 10, 5214, <https://doi.org/10.1038/s41467-019-12982-0>, 2019.
- 394 Luo, Q. W., Hong, J., Xu, H. B., Han, S., Tan, H. B., Wang, Q. Q., Tao, J. C., Ma, N., Cheng, Y. F., and Su, H.: Hygroscopicity  
395 of amino acids and their effect on the water uptake of ammonium sulfate in the mixed aerosol particles, *Sci. Total Environ.*,  
396 734, 139318, <https://doi.org/10.1016/j.scitotenv.2020.139318>, 2020.
- 397 Metcalf, A. R., Boyer, H. C., and Dutcher, C. S.: Interfacial tensions of aged organic aerosol particle mimics using a biphasic  
398 microfluidic platform, *Environ. Sci. Technol.*, 50, 1251-1259, <https://doi.org/10.1021/acs.est.5b04880>, 2016.
- 399 Minambres, L., Mendez, E., Sanchez, M. N., Castano, F., and Basterretxea, F. J.: Water uptake of internally mixed ammonium  
400 sulfate and dicarboxylic acid particles probed by infrared spectroscopy, *Atmos. Environ.*, 70, 108-116,  
401 <https://doi.org/10.1016/j.atmosenv.2013.01.007>, 2013.
- 402 Moore, R. H. and Nenes, A.: Scanning Flow CCN Analysis—A Method for Fast Measurements of CCN Spectra, *Aerosol Sci.*  
403 *Technol.*, 43, 1192-1207, <https://doi.org/10.1080/02786820903289780>, 2009.
- 404 Morris, H. S., Grassian, V. H., and Tivanski, A. V.: Humidity-dependent surface tension measurements of individual inorganic  
405 and organic submicrometre liquid particles, *Chem. Sci.*, 6, 3242-3247, <https://doi.org/10.1039/c4sc03716b>, 2015.
- 406 Nguyen, Q. T., Kjær, K. H., Kling, K. I., Boesen, T., and Bilde, M.: Impact of fatty acid coating on the CCN activity of sea  
407 salt particles, *Tellus B: Chem. Phys. Meteorol.*, 69, <https://doi.org/10.1080/16000889.2017.1304064>, 2017.



- 408 Ovadnevaite, J., Zuend, A., Laaksonen, A., Sanchez, K. J., Roberts, G., Ceburnis, D., Decesari, S., Rinaldi, M., Hodas, N.,  
409 Facchini, M. C., Seinfeld, J. H., and C, O. D.: Surface tension prevails over solute effect in organic-influenced cloud droplet  
410 activation, *Nature*, 546, 637-641, <https://doi.org/10.1038/nature22806>, 2017.
- 411 Pajunoja, A., Lambe, A. T., Hakala, J., Rastak, N., Cummings, M. J., Brogan, J. F., Hao, L. Q., Paramonov, M., Hong, J.,  
412 Prisle, N. L., Malila, J., Romakkaniemi, S., Lehtinen, K. E. J., Laaksonen, A., Kulmala, M., Massoli, P., Onasch, T. B.,  
413 Donahue, N. M., Riipinen, I., Davidovits, P., Worsnop, D. R., Petaja, T., and Virtanen, A.: Adsorptive uptake of water by  
414 semisolid secondary organic aerosols, *Geophys. Res. Lett.*, 42, 3063-3068, <https://doi.org/10.1002/2015gl063142>, 2015.
- 415 Parsons, M. T., Mak, J., Lipetz, S. R., and Bertram, A. K.: Deliquescence of malonic, succinic, glutaric, and adipic acid  
416 particles, *J. Geophys. Res.: Atmos.*, 109, D06212, <https://doi.org/10.1029/2003jd004075>, 2004.
- 417 Peng, C., Chan, M. N., and Chan, C. K.: The hygroscopic properties of dicarboxylic and multifunctional acids: Measurements  
418 and UNIFAC predictions, *Environ. Sci. Technol.*, 35, 4495-4501, <https://doi.org/10.1021/es0107531>, 2001.
- 419 Peng, C., Jing, B., Guo, Y. C., Zhang, Y. H., and Ge, M. F.: Hygroscopic behavior of multicomponent aerosols involving NaCl  
420 and dicarboxylic Acids, *J. Phys. Chem. A*, 120, 1029-1038, <https://doi.org/10.1021/acs.jpca.5b09373>, 2016.
- 421 Peng, C., Razafindrambinina, P. N., Malek, K. A., Chen, L. X. D., Wang, W. G., Huang, R. J., Zhang, Y. Q., Ding, X., Ge, M.  
422 F., Wang, X. M., Asa-Awuku, A. A., and Tang, M. J.: Interactions of organosulfates with water vapor under sub- and  
423 supersaturated conditions, *Atmos. Chem. Phys.*, 21, 7135-7148, <https://doi.org/10.5194/acp-21-7135-2021>, 2021.
- 424 Peng, C., Chen, L., and Tang, M.: A database for deliquescence and efflorescence relative humidities of compounds with  
425 atmospheric relevance, *Fundam. Res.*, 2, 578-587, <https://doi.org/10.1016/j.fmre.2021.11.021>, 2022.
- 426 Petters, M. D. and Kreidenweis, S. M.: A single parameter representation of hygroscopic growth and cloud condensation  
427 nucleus activity, *Atmos. Chem. Phys.*, 7, 1961-1971, <https://doi.org/10.5194/acp-7-1961-2007>, 2007.
- 428 Petters, M. D., Kreidenweis, S. M., Prenni, A. J., Sullivan, R. C., Carrico, C. M., Koehler, K. A., and Ziemann, P. J.: Role of  
429 molecular size in cloud droplet activation, *Geophys. Res. Lett.*, 36, <https://doi.org/10.1029/2009gl040131>, 2009.
- 430 Petters, S. S., Pagonis, D., Claflin, M. S., Levin, E. J. T., Petters, M. D., Ziemann, P. J., and Kreidenweis, S. M.: Hygroscopicity  
431 of organic compounds as a function of carbon chain length and carboxyl, hydroperoxy, and carbonyl functional groups, *J. Phys.*  
432 *Chem. A*, 121, 5164-5174, <https://doi.org/10.1021/acs.jpca.7b04114>, 2017.
- 433 Ray, K. K., Lee, H. D., Gutierrez, M. A., Jr., Chang, F. J., and Tivanski, A. V.: Correlating 3D morphology, phase state, and  
434 viscoelastic properties of individual substrate-deposited particles, *Anal. Chem.*, 91, 7621-7630,  
435 <https://doi.org/10.1021/acs.analchem.9b00333>, 2019.
- 436 Römpp, A., Winterhalter, R., and Moortgat, G. K.: Oxodicarboxylic acids in atmospheric aerosol particles, *Atmos. Environ.*,  
437 40, 6846-6862, <https://doi.org/10.1016/j.atmosenv.2006.05.053>, 2006.
- 438 Rose, D., Gunthe, S. S., Mikhailov, E., Frank, G. P., Dusek, U., Andreae, M. O., and Pöschl, U.: Calibration and measurement  
439 uncertainties of a continuous-flow cloud condensation nuclei counter (DMT-CCNC): CCN activation of ammonium sulfate  
440 and sodium chloride aerosol particles in theory and experiment, *Atmos. Chem. Phys.*, 8, 1153-1179,  
441 <https://doi.org/10.5194/acp-8-1153-2008>, 2008.





- 442 Rose, D., Nowak, A., Achtert, P., Wiedensohler, A., Hu, M., Shao, M., Zhang, Y., Andreae, M. O., and Pöschl, U.: Cloud  
443 condensation nuclei in polluted air and biomass burning smoke near the mega-city Guangzhou, China – Part I: Size-resolved  
444 measurements and implications for the modeling of aerosol particle hygroscopicity and CCN activity, *Atmos. Chem. Phys.*,  
445 10, 3365-3383, <https://doi.org/10.5194/acp-10-3365-2010>, 2010.
- 446 Rosenfeld, D., Sherwood, S., Wood, R., and Donner, L.: Climate effects of aerosol-cloud interactions, *Science*, 343, 379-380,  
447 <https://doi.org/10.1126/science.1247490>, 2014.
- 448 Ruehl, C. R., Chuang, P. Y., and Nenes, A.: Aerosol hygroscopicity at high (99 to 100%) relative humidities, *Atmos. Chem.*  
449 *Phys.*, 10, 1329-1344, <https://doi.org/10.5194/acp-10-1329-2010>, 2010.
- 450 Ruehl, C. R., Chuang, P. Y., Nenes, A., Cappa, C. D., Kolesar, K. R., and Goldstein, A. H.: Strong evidence of surface tension  
451 reduction in microscopic aqueous droplets, *Geophys. Res. Lett.*, 39, L23801, <https://doi.org/10.1029/2012gl053706>, 2012.
- 452 Ruehl, C. R. and Wilson, K. R.: Surface organic monolayers control the hygroscopic growth of submicrometer particles at  
453 high relative humidity, *J. Phys. Chem. A*, 118, 3952-3966, <https://doi.org/10.1021/jp502844g>, 2014.
- 454 Ruehl, C. R., Davies, J. F., and Wilson, K. R.: An interfacial mechanism for cloud droplet formation on organic aerosols,  
455 *Science*, 351, 1447-1450, <https://doi.org/10.1126/science.aad4889>, 2016.
- 456 Shiraiwa, M., Li, Y., Tsimpidi, A. P., Karydis, V. A., Berkemeier, T., Pandis, S. N., Lelieveld, J., Koop, T., and Poschl, U.:  
457 Global distribution of particle phase state in atmospheric secondary organic aerosols, *Nat. Commun.*, 8, 15002,  
458 <https://doi.org/10.1038/ncomms15002>, 2017.
- 459 Sjogren, S., Gysel, M., Weingartner, E., Baltensperger, U., Cubison, M. J., Coe, H., Zardini, A. A., Marcolli, C., Krieger, U.  
460 K., and Peter, T.: Hygroscopic growth and water uptake kinetics of two-phase aerosol particles consisting of ammonium sulfate,  
461 adipic and humic acid mixtures, *J. Aerosol Sci.*, 38, 157-171, <https://doi.org/10.1016/j.jaerosci.2006.11.005>, 2007.
- 462 Suda, S. R., Petters, M. D., Yeh, G. K., Strollo, C., Matsunaga, A., Faulhaber, A., Ziemann, P. J., Prenni, A. J., Carrico, C. M.,  
463 Sullivan, R. C., and Kreidenweis, S. M.: Influence of functional groups on organic aerosol cloud condensation nucleus activity,  
464 *Environ. Sci. Technol.*, 48, 10182-10190, <https://doi.org/10.1021/es502147y>, 2014.
- 465 Vepsäläinen, S., Calderón, S. M., Malila, J., and Prisle, N. L.: Comparison of six approaches to predicting droplet activation  
466 of surface active aerosol – Part 1: moderately surface active organics, *Atmos. Chem. Phys.*, 22, 2669-2687,  
467 <https://doi.org/10.5194/acp-22-2669-2022>, 2022.
- 468 Wu, Z. J., Poulain, L., Henning, S., Dieckmann, K., Birmili, W., Merkel, M., van Pinxteren, D., Spindler, G., Müller, K.,  
469 Stratmann, F., Herrmann, H., and Wiedensohler, A.: Relating particle hygroscopicity and CCN activity to chemical  
470 composition during the HCCT-2010 field campaign, *Atmos. Chem. Phys.*, 13, 7983-7996, <https://doi.org/10.5194/acp-13-7983-2013>, 2013.
- 472 Yazdanpanah, M. M., Hosseini, M., Pabba, S., Berry, S. M., Dobrokhoto, V. V., Safir, A., Keynton, R. S., and Cohn, R. W.:  
473 Micro-wilhelmy and related liquid property measurements using constant-diameter nanoneedle-tipped atomic force  
474 microscope probes, *Langmuir*, 24, 13753-13764, <https://doi.org/10.1021/la802820u>, 2008.



475 Zhang, C., Bu, L., Fan, F., Ma, N., Wang, Y., Yang, Y., Größ, J., Yan, J., and Wiedensohler, A.: Surfactant effect on the  
476 hygroscopicity of aerosol particles at relative humidity ranging from 80% to 99.5%: Internally mixed adipic acid-ammonium  
477 sulfate particles, *Atmos. Environ.*, 266, 118725–118736, <https://doi.org/10.1016/j.atmosenv.2021.118725>, 2021.

478 Zhang, Y., Tao, J., Ma, N., Kuang, Y., Wang, Z., Cheng, P., Xu, W., Yang, W., Zhang, S., Xiong, C., Dong, W., Xie, L., Sun,  
479 Y., Fu, P., Zhou, G., Cheng, Y., and Su, H.: Predicting cloud condensation nuclei number concentration based on conventional  
480 measurements of aerosol properties in the North China Plain, *Sci. Total Environ.*, 719, 137473,  
481 <https://doi.org/10.1016/j.scitotenv.2020.137473>, 2020.

482 Zhao, D. F., Buchholz, A., Kortner, B., Schlag, P., Rubach, F., Fuchs, H., Kiendler-Scharr, A., Tillmann, R., Wahner, A.,  
483 Watne, Å. K., Hallquist, M., Flores, J. M., Rudich, Y., Kristensen, K., Hansen, A. M. K., Glasius, M., Kourtchev, I., Kalberer,  
484 M., and Mentel, T. F.: Cloud condensation nuclei activity, droplet growth kinetics, and hygroscopicity of biogenic and  
485 anthropogenic secondary organic aerosol (SOA), *Atmos. Chem. Phys.*, 16, 1105-1121, [https://doi.org/10.5194/acp-16-1105-](https://doi.org/10.5194/acp-16-1105-2016)  
486 2016, 2016.

487

488



489 **Table 1. Substances and their relevant properties investigated in this study.**

Compounds	Molar weight (g mol <sup>-1</sup> )	Density (g cm <sup>-3</sup> )	Solubility (g L <sup>-1</sup> )	DRH (%RH)	Purity	Supplier
NaCl	58.44 <sup>a</sup>	2.16 <sup>a</sup>	360 <sup>b</sup>	73-77 <sup>c</sup>	GR	Sinopharm Chemical Reagent
AS	132.13 <sup>a</sup>	1.77 <sup>a</sup>	770 <sup>b</sup>	78-82 <sup>c</sup>	≥99%	Sigma Aldrich
MA	104.06 <sup>a</sup>	1.63 <sup>a</sup>	1400 <sup>b</sup>	65-76 <sup>c</sup>	≥99%	Sigma Aldrich
PhMA	180.16 <sup>a</sup>	1.40 <sup>a</sup>	131 <sup>a</sup>	NA	98%	Aladdin
SA	118.09 <sup>a</sup>	1.57 <sup>a</sup>	80 <sup>b</sup>	98 <sup>d</sup>	≥99%	Aladdin
PhSA	194.19 <sup>a</sup>	1.13 <sup>a</sup>	241 <sup>a</sup>	NA	98%	Macklin
AA	146.14 <sup>a</sup>	1.36 <sup>a</sup>	14.4 <sup>b</sup>	~100 <sup>c</sup>	GR	Sinopharm Chemical Reagent
PA	160.17 <sup>a</sup>	1.28 <sup>a</sup>	25 <sup>b</sup>	>90 <sup>c</sup>	99%	Macklin
OA	174.20 <sup>a</sup>	1.16 <sup>a</sup>	12 <sup>a</sup>	>90 <sup>c</sup>	99%	Aladdin

490 <sup>a</sup> <https://comptox.epa.gov/> (last access: 3rd August 2022). <sup>b</sup> <https://www.chemicalbook.com/> (last access: 3rd August 2022). <sup>c</sup>  
 491 Peng et al. (2022) and references therein. <sup>d</sup> Peng et al. (2001). <sup>e</sup> Parsons et al. (2004). DRH means deliquescence RH. GR  
 492 means guaranteed reagent. NA indicates no reported results are available.

493

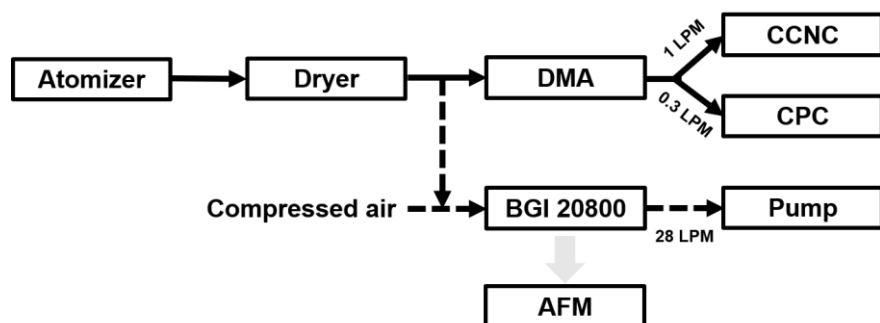
494 **Table 2. Summary of  $\kappa_{CCN}$  for single component particles.**

Chemicals	$D_d$ (nm)	$\kappa_{CCN}$	Previous reported $\kappa_{CCN}$
		mean ± standard deviation	
NaCl	50, 65, 76, 88, 100	1.325 ± 0.038	1.28 <sup>a</sup>
AS	50, 65, 76, 88, 100	0.562 ± 0.059	0.61 <sup>a</sup>
MA	50, 65, 76, 88, 100	0.240 ± 0.036	0.227 <sup>a</sup>
PhMA	50, 65, 76, 88, 100	0.183 ± 0.032	This study
SA	50, 65, 76, 88, 100	0.204 ± 0.023	0.166-0.295 <sup>a</sup>
PhSA	50, 65, 76, 88, 100	0.145 ± 0.017	This study
AA	140, 160, 180, 200	0.008 ± 0.001	0.005-0.008 <sup>b</sup>
PA	65, 76, 88, 100	0.112 ± 0.010	0.14 <sup>b</sup>
OA	200, 220, 240, 260	0.003 ± 0.0002	0.001 <sup>b</sup>

495 <sup>a</sup> Petters et al., 2007; <sup>b</sup> Kuwata et al. (2013) and references therein.

496

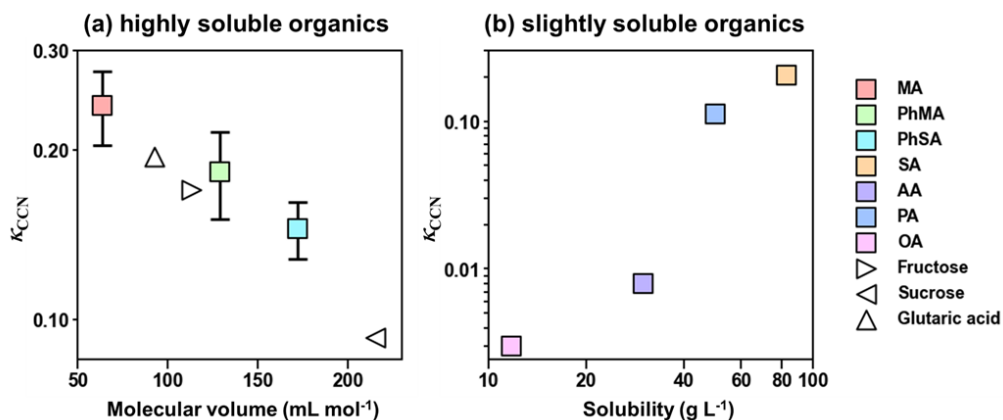
497



498

499 **Figure 1:** Schematic illustration of the instrumental set-up. The arrow indicates the flow direction. LPM means liter per minute.

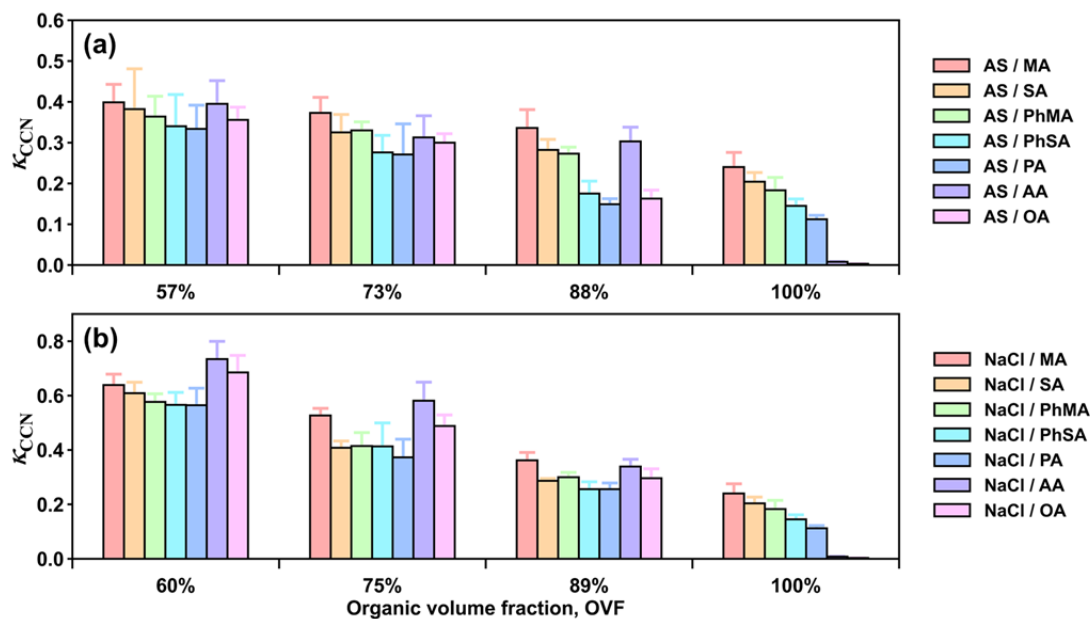
500



501

502 **Figure 2:**  $\kappa_{CCN}$  of organic compounds as a function of (a) molecular volume and (b) solubility. Solid squares represent  $\kappa_{CCN}$  results  
503 in this study while hollow triangles were  $\kappa_{CCN}$  results obtained from Chan et al. (2008).

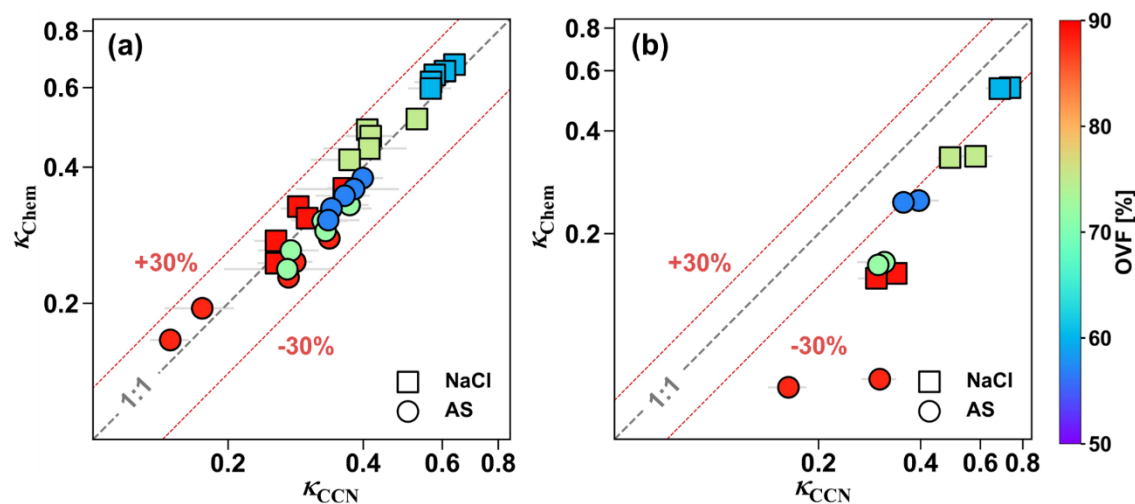
504



505

506 Figure 3:  $\kappa_{CCN}$  of (a) AS/dicarboxylic acid and (b) NaCl/dicarboxylic acid mixed particles with varied OVF.

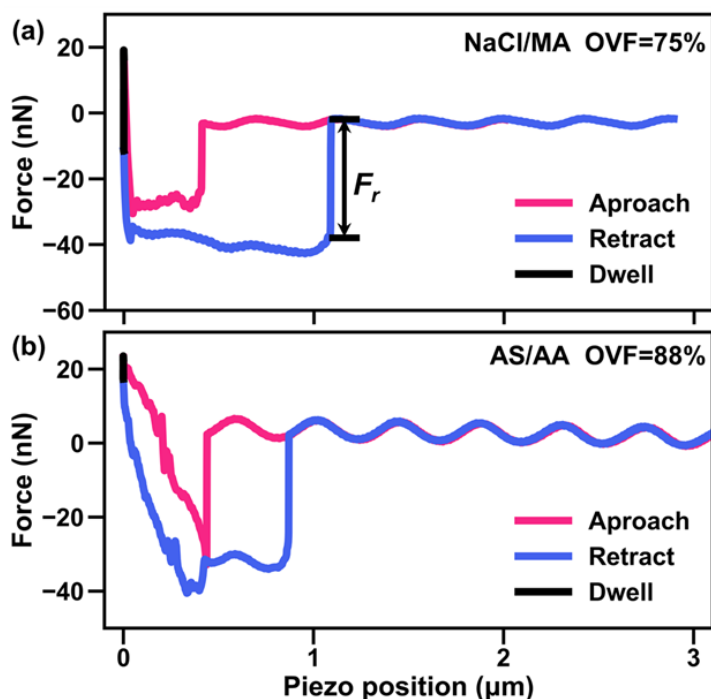
507



508

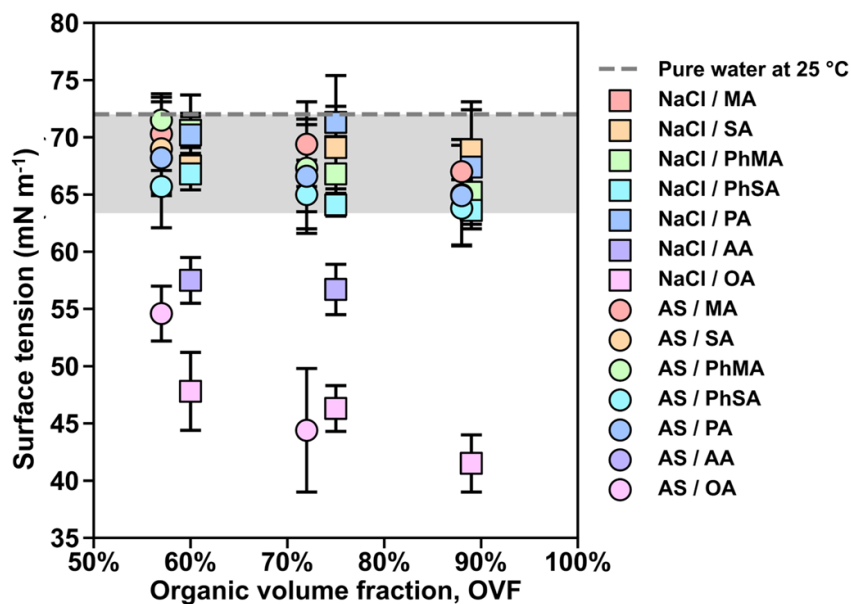
509 Figure 4: Comparison between  $\kappa_{CCN}$  and  $\kappa_{Chem}$  of (a) inorganic salt mixed with MA, PhMA, SA, PhSA and PA (b) inorganic salt  
 510 mixed with AA and OA. Square represents NaCl containing particles and circle represents AS containing particles. Color bar  
 511 indicates OVF.

512



513

514 Figure 5: AFM force plots of (a) NaCl/MA system with 75% OVF and (b) AS/AA system with 88% OVF.  $F_r$  is the retention force to  
 515 break the meniscus by the tip of AFM probe.



516

517 Figure 6: Measured surface tension values of inorganic salt/dicarboxylic acid particles under RH over 99.5%. Gray area covers the  
 518 surface tension reductions below 12% comparing with pure water ( $72 \text{ mN m}^{-1}$ ).

519